Knee Surg Sports Traumatol Arthrosc
DOI 10.1007/s00167-010-1281-3

KNEE

Axial and torsional stability of supracondylar femur osteotomies: biomechanical comparison of the stability of five different plate and osteotomy configurations

J.-M. Brinkman · C. Hurschler · J. D. Agneskirchner · D. Freiling · R. J. van Heerwaarden

Received: 16 February 2010 / Accepted: 15 September 2010

Abstract
Purpose Little is known regarding the biomechanical stability and stiffness of implants and techniques used in supracondylar femur osteotomies (SCO). Therefore, fixation stability and stiffness of implants to bone was investigated under simulated physiological loading conditions using a composite femur model and a 3D motion-analysis system.
Methods Five osteotomy configurations were investigated: (1) oblique medial closing-wedge fixated with an angle-stable implant; (2) oblique and (3) perpendicular medial closing-wedge, both fixated with an angled blade plate; and lateral opening-wedge fixated with (4) a spacer plate and (5) an angle-stable lateral implant. The motion measured at the osteotomy was used to calculate the stiffness and stability of the constructs.
Results The least amount of motion and highest stiffness was measured in the medial oblique closing-wedge osteotomy fixated with the angled blade plate. The lateral opening-wedge techniques were less stable and had a lower stiffness compared with the medial; the oblique saw cuts were more stable and had a higher stiffness than the perpendicular.
Conclusion This experimental study presents baseline data on the differences in the primary stability of bone–implant constructs used in SCO. The data in this study can be used as reference for future testing of SCO techniques. Furthermore, it is recommended that based on the differences found, the early postoperative rehabilitation protocol is tailored to the stability and stiffness of the fixation method used.

Keywords Distal femur · Osteotomy technique · Primary stability

J.-M. Brinkman (✉) · R. J. van Heerwaarden
Department of Orthopaedics, Limb Deformity Reconstruction Unit, Sint Maartenskliniek, P.O. Box 8000, 3440 JD Woerden, The Netherlands
e-mail: justusmartijn@gmail.com

C. Hurschler
Laboratory for Biomechanics und Biomaterials, Orthopaedic Department, Hannover Medical School, Anna-von-Borries-Strasse 1-7, 30625 Hannover, Germany

J. D. Agneskirchner · D. Freiling
Department of Trauma and Reconstructive Surgery, Henriettenstiftung, Marienstrasse 72-90, 30171 Hannover, Germany

Introduction

Distal femoral supracondylar osteotomy (SCO) is a well-established surgical procedure for the treatment of lateral compartment osteoarthritis of the knee with a valgus leg alignment [6, 11, 13, 16–18]. Stability of the plate and osteotomy construct after SCO is crucial in order to retain the achieved correction during functional postoperative rehabilitation. An oblique closing-wedge osteotomy direction has been suggested to enhance stability [17]. Devices used for the fixation of supracondylar fractures have been previously investigated biomechanically using both cadaver and composite bone [3, 5, 25]. The artificial bones used provided reproducible bone properties and allowed the circumvention of the problems of availability and inter-specimen variability associated with cadaver specimens. The structural equivalence of these composite femurs with human bones has been validated [9, 22].

In this study, the stability and stiffness of four implant devices for opening-wedge and closing-wedge SCO techniques were tested. Simulated physiological loading and

Published online: 07 October 2010

subsequent loading to failure were applied using a material testing machine (MTS), and osteosynthesis gap measurements were performed using a three-dimensional (3D) motion-analysis system. The specific research goals of the study were to compare (1) the standard medial closing-wedge SCO technique using an angled blade plate and rigid compression and a new medial distal femur plate based on the locking compression plate (LCP) principles [8], (2) the lateral opening-wedge technique using both a conventional and an LCP lateral distal femur plate and closing-wedge techniques and (3) the medial closing-wedge oblique SCO and medial closing-wedge perpendicular SCO technique.

Materials and methods

Thirty short-glass-fibre-reinforced (SGFR) third-generation composite replicate femurs (Sawbones Europe AB, Malmö, Sweden) were used in five test modalities: (1) ABPobl: oblique medial closing-wedge SCO with a 90°-angled blade plate (AO/ASIF, Davos, Swiss), (2) MDF: oblique medial closing-wedge SCO with a medial LCP (Tomofix, Synthes, Bettlach, Swiss), (3) ASP: lateral opening-wedge SCO with a non-angle-stable spacer plate (Arthrex spacer plate, Naples, FL, USA), (4) LDF: lateral opening-wedge SCO with a lateral LCP (Tomofix, Synthes, Bettlach, Switzerland) and (5) ABPperp: perpendicular medial closing-wedge SCO with a 90°-angled blade plate (AO/ASIF, Davos, Swiss) (Fig. 1 and Table 1). Six femurs were available for each test modality, 3 for axial testing and 3 for torsional testing; all 30 femurs were subsequently tested to failure (Table 1).

Experimental set-up

The osteotomies were performed, and the plates implanted according to the standard surgical procedure for each implant. A wedge of 10° was either removed in the closing-wedge SCO or created in the opening-wedge SCO. To achieve this, all composite femurs were aligned in a standardized way using an alignment jig and a femur saw guide (Balansys®, Mathys Medical, Bettlach, Swiss) that provided a reproducible osteotomy position, osteotomy direction and wedge size. The lateral opening-wedge and the oblique medial closing-wedge were directed 20° oblique to the distal femur condylar line, whereas the medial perpendicular wedge was directed parallel to the distal femur condyles. The bone deformation needed for the opening or closing of the wedge and the implant fixation were performed without producing a fracture in the opposite bone bridge. The femur head and trochanter and the distal femur end were thereafter embedded in a polyurethane-based cold-curing resin (Ureol FC 53, Vantico GmbH, Wehr, Germany) in a specially constructed fixture; the fixture allowed for mounting of the femur in a materials testing machine (MTS)(Mini Bionix, MTS Systems Corporation, Eden Prairie, MN, USA) (Fig. 2). The fixture was designed in such a way that the axis of loading of the replicate femur in the MTS was through the centre of the femur head proximal and through a point 18-mm medial from the mid-condylar distance, creating a mechanical femur axis of 2°; reproducing loading in the normally aligned human knee after a SCO for valgus osteoarthritis [10, 12] (Fig. 2). The fixture allowed the MTS to apply both an axial load along and a torsion load around the mechanical axis of the femur (Fig. 2).

Measuring system

The principles of rigid body motion were used to measure (micro) motion across the SCO. Reference point pairs, relative to which motion was measured, were defined on the replicate femur both proximal and distal to the osteotomy gap; two points across the midpoint of the intact cortical bridge, two points midway across the osteotomy at the level of the deepest point of the trochlea and two points just posterior of the plate on the femur. Motion (displacement)

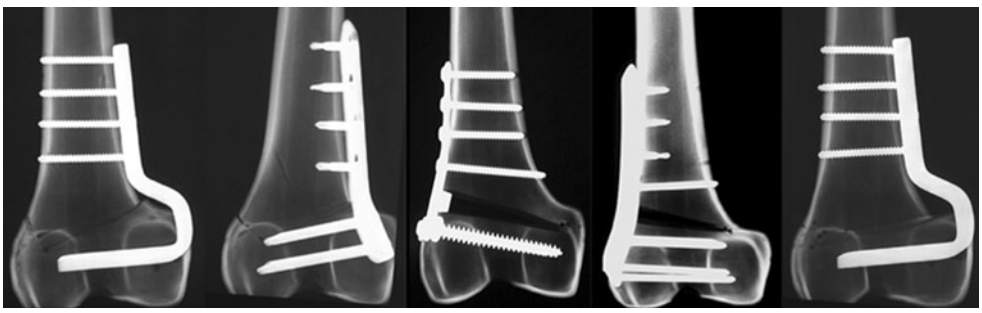

Fig. 1 Overview of the five configurations. AP radiographs of all implants, from *left* to *right*: *ABPobl* angled blade plate oblique osteotomy, *MDF* angle-stable implant oblique osteotomy, *ASP* non-angle-stable lateral implant, *LDF* angle-stable lateral implant and *ABPperp* angled blade plate perpendicular osteotomy

Table 1 Overview of the configurations and test protocols

Total no.	Implant type	SCO technique	No femurs	Test runs per femur	Cycles	Axial pre-load	Loading	Torsional pre-load	Loading
	Axial loading			*Axial loading*					
15	Blade plate	Oblique	3	1	100	10 N	150 N	–	–
	Blade plate	Perpendicular	3	2	100	10 N	800 N	–	–
	MDF	Oblique	3	3	1	–	Failure	–	–
	LDF	Lateral open	3						
	ASP	Lateral open	3						
	Torsional loading			*Torsional loading*					
15	Blade plate	Oblique	3	1	100	–	–	0.5 Nm	5 Nm
	Blade plate	Perpendicular	3	2	100	150 N	–	0.5 Nm	5 Nm
	MDF	Oblique	3	3	100	800 N	–	0.5 Nm	5 Nm
	LDF	Lateral open	3	4	1	–	–	–	Failure
	ASP	Lateral open	3						

An overview of the number of femurs, the different implants and SCO techniques (left) and loading protocols that were used in the tests is shown (right)

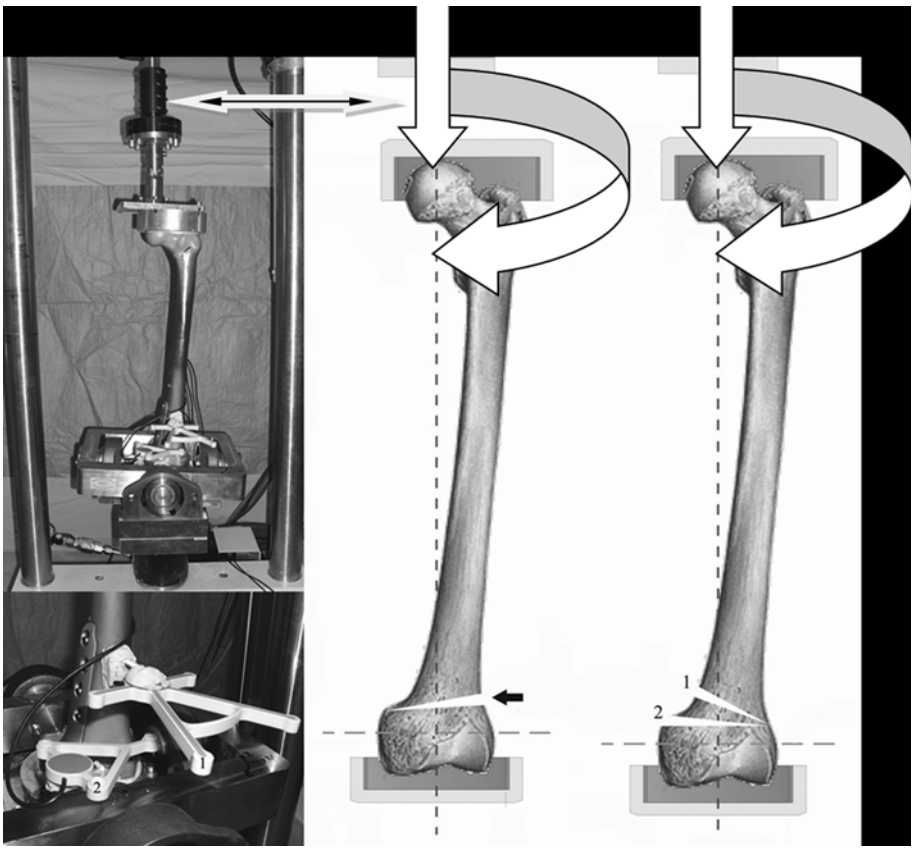

Fig. 2 Schematic and actual view of the test setup. *Top left* the setup in the MTS. *Bottom left* close up of the 3D measuring system; *1* and *2*, microphone and speaker. *Right* corresponding schematic view of the setup and loading axis used in the MTS, a loading axis just medial from the mid-condylar distance is used, corresponding with a mechanical loading axis of 2° varus. The *white arrows* show the direction of force applied by the top half of the MTS. Also shown are the lateral open wedge osteotomy (*black arrow*), and the (*1*) Oblique osteotomy and (*2*) Perpendicular osteotomy

of the diaphysis of the femur proximal to the osteotomy was measured relative to the femur condyles distal to the osteotomy using an ultrasound 3D motion-analysis system (CMS20S, Zebris Medizintechnik, GmbH, Isny, Germany). This system is based on the travel time measurement of ultrasonic pulses that are emitted by miniature speakers on a marker-triplet to microphones on a second marker-quartet (Fig. 2). Its use has been validated in cervical spine kinematics analysis [4, 24]. Its current use has, to the best of our knowledge, not been documented previously. The accuracy of the system as reported by the manufacturer is 0.01 mm (Zebris Medizintechnik, GmbH, Isny, Germany).

The sensor and emitter markers were rigidly fixed to the femur using bone cement (Palacos, Biomet, Inc, Warsaw, IN, USA). After mounting of the femur in the MTS with the microphone template attached, a coordinate system was defined based on landmarks on the distal femur using a calibrated pointer device temporarily attached to the emitter-marker. The coordinate axes were defined in such a way that the anatomical medial–lateral axis corresponded to the *Y*-axis, the anterior posterior axis to the *X*-axis and the proximal–distal axis to the *Z*-axis. The coordinates of the point pairs relative to which motion was measured were then registered. Before the start of the loading cycles, the MTS was first calibrated to the 0 position, meaning it was not putting any pressure on the loaded femur. In this state, the Zebris system was calibrated to the 0 position. This process was repeated for each femur for each test run. During testing, the motion-analysis system continuously measured displacement at a rate of 20 Hz. Force and moment data were recorded by the materials testing machine at a rate of 20 Hz.

Loading protocol

The replicate femurs were subjected to axial and torsional loading protocols designed to simulate physiological loading (Table 1). Cyclical axial loading was performed at two loading levels (150 and 800 N) on 3 femurs per SCO configuration simulating partial and full weight bearing in an 80-kg patient. After an axial preload of 10 N was achieved, the femurs were tested during 100 cycles for each load at a rate of 0.5 Hz.

Each femur was subsequently tested to failure under displacement control at a rate of 0.1 mm per second. Failure was defined by a drop of actuator loading, either because of failure of the bone, bone–implant construct, or of the implant itself.

Cyclical torsional loading was also performed in 3 femurs per SCO modality using a 0.5 Nm torsional preload. Internal rotation around the *Z*-axis with a cyclical moment loading of 5 Nm at a rate of 0.25 Hz was applied during 100 cycles, with an increasing axial pre-load (Table 1). The different axial preloads were used to simulate no, partial and full weight bearing. After completion of all three runs, each femur was tested to failure under displacement control at a rate of 0.25° per second. Criteria for failure were the same as used for the axial loading failure tests.

Statistical analysis

The displacement data recorded were computed using a custom-written programme in Mathematica (version 5.0, Wolfram research, Inc, Champaign, IL, USA); the change in position and the angle of rotation around all axes for each measuring point and the change in absolute distance between the measuring points were calculated. Displacement at the SCO was calculated using the change in the (absolute) distance between the measuring points per loading cycle. The amount of motion that occurs at the SCO was defined as the difference between the maximum increase and maximum decrease in the distance between measuring points; determined for each cycle and per measuring point. A greater mean difference calculated over 100 cycles and 3 measuring points indicates more motion allowed by the bone–implant construct. Stability was subsequently defined as the amount of motion allowed by the construct.

A similar approach was used in the torsional tests. The amount of motion was calculated by determining the amount of rotation around the *Z*-axis that is allowed by the bone–implant construct during each cycle. Stability in torsion was defined as the amount of rotation allowed by the construct.

The stiffness under axial compression of the construct was calculated by plotting displacement at the SCO during the failure test, defined as the average amount of movement on the *Z*-axis of the 3 previously defined point pairs, against the force data. Stiffness of the bone–implant construct was defined as the slope of the linear portion of the force-osteotomy deformation curve (i.e. the force required per millimetre of displacement). Stiffness under torsion loading was calculated by plotting the rotation around the *Z*-axis over time against the moment (Nm) applied by the MTS and defined as Nm required for one degree of rotation.

Statistical analysis was performed using SPSS statistical software (Version 11.5, SPSS, Inc, Chicago, IL, USA); one-way ANOVA was used to measure statistical differences between modalities, and P values < 0.05 were considered significant using a 95% confidence interval (CI_{95}).

Results

Axial loading

No visible damage to bone, bone–implant construct or implant was found during the axial loading tests. During each cycle of loading and unloading, a corresponding movement at the osteotomy was observed to occur.

The displacement data showed that there were varying differences between the configurations tested (Table 2 and Fig. 3).

The oblique OT (ABPobl) allowed significantly less motion than the perpendicular OT (ABPperp) in the 800 N test (Table 3). ABPobl compared with MDF allowed less

Table 2 Axial and torsion test results

	OT type	Preload	Axial load	N	Mean	SD ±	95% CI for mean		Min	Max
							Lower–upper bound			
Axial										
	ABPobl		150 N	300	0.057	0.038	0.052	0.061	0	0.143
	MDF			300	0.070	0.043	0.065	0.075	0	0.256
	ASP			300	0.094	0.046	0.089	0.100	0	0.239
	LDF			300	0.068	0.044	0.063	0.073	0	0.226
	ABPperp			300	0.038	0.065	0.030	0.045	0	0.178
	ABPobl		800 N	300	0.100	0.043	0.095	0.105	0.057	0.720
	MDF			300	0.105	0.030	0.101	0.108	0.037	0.183
	ASP			300	0.170	0.034	0.166	0.173	0.093	0.336
	LDF			300	0.108	0.025	0.106	0.111	0.013	0.191
	ABPperp			300	0.112	0.032	0.109	0.116	0	0.241
Torsion										
	ABPobl	0 N		300	0.049	0.018	0.047	0.051	0.009	0.136
	MDF			300	0.053	0.017	0.051	0.055	0.015	0.111
	ASP			300	0.043	0.018	0.041	0.045	0.010	0.093
	LDF			300	0.055	0.016	0.053	0.057	0.017	0.114
	ABPperp			300	0.060	0.026	0.057	0.063	0.020	0.158
	ABPobl	150 N		300	0.042	0.014	0.041	0.044	0.014	0.079
	MDF			300	0.045	0.018	0.043	0.047	0.006	0.104
	ASP			300	0.052	0.021	0.049	0.054	0.011	0.093
	LDF			300	0.047	0.014	0.045	0.048	0.011	0.084
	ABPperp			300	0.061	0.013	0.060	0.062	0.030	0.102
	ABPobl	800 N		300	0.041	0.015	0.040	0.043	0.000	0.082
	MDF			300	0.044	0.015	0.042	0.045	0.014	0.130
	ASP			300	0.045	0.017	0.043	0.047	0.010	0.094
	LDF			300	0.053	0.017	0.051	0.055	0.014	0.094
	ABPperp			300	0.056	0.015	0.054	0.058	0.022	0.095

Results for the axial and torsion tests are shown; osteotomy type, axial load, total number of cycles and the mean displacement, including the standard deviation (SD), CI_{95} and minimum and maximum, are detailed

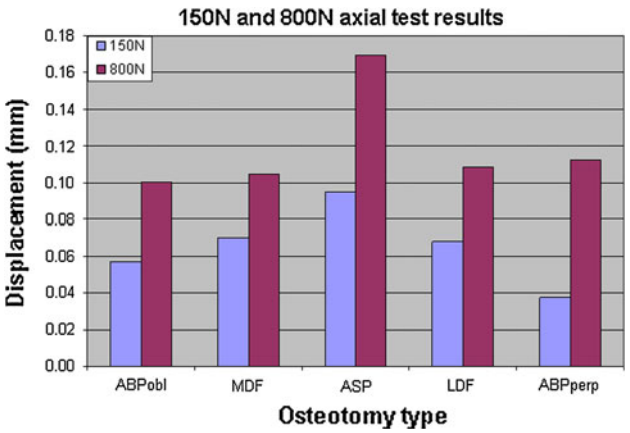

Fig. 3 Graphic view of the axial test results. Results for both the 150 and 800 N axial compression tests; results for each test is displayed for each modality; displacement is displayed in millimetres (mm)

motion in all tests, but to a significant level only in the 150 N axial tests (Table 3).

Axial failure tests

All 15 failure tests resulted in a per-trochanteric femoral neck failure; failure occurred proximally to the osteotomy. No macroscopically observable failure at the bone–implant interface or of the implant itself was observed. Fracture of the medial opposite cortex bone-bridge occurred during the failure test in all ASP femurs, as well as in 1 LDF. No fractures of the opposing lateral cortex bone-bridge were observed in the medial closing-wedge SCOs. During the axial failure tests, the force time course of loading typically demonstrated an increasing axial compression load with a sudden drop in load at failure. Calculated stiffness was

Table 3 Statistical comparison of the axial and torsion test results

		Axial tests		Torsion tests			Axial tests		Torsion tests		
		150 N	800 N	0 N	150 N	800 N	150 N	800 N	0 N	150 N	800 N
ABPobl	MDF	>	>	>	>	>	0.0001	–	–	–	–
	ASP	>	>	<	>	>	0.0001	0.0001	0.001	0.0001	–
	LDF	>	>	>	>	>	0.035	0.03	0.004	0.014	0.0001
	ABPperp	<	>	>	>	>	0.0001	0.0001	0.0001	0.0001	0.0001
MDF	ASP	>	>	<	>	>	0.0001	0.0001	0.0001	0.0001	–
	LDF	>	>	>	>	>	–	–	–	–	0.0001
	ABPperp	<	>	>	>	>	0.0001	0.038	0.0002	0.0001	0.0001
ASP	LDF	<	<	>	<	>	0.0001	0.0001	0.0001	0.002	0.0001
	ABPperp	<	<	>	>	>	0.0001	0.0001	0.0001	0.0001	0.0001
LDF	ABPperp	<	<	>	>	>	0.0001	–	0.009	0.0001	–

The motion data of each configuration are compared with the other configurations. On the left, the arrows indicate which configuration is more stable, and on the right, the statistical level of significance of the differences is shown

For example, the first row shows that the ABPobl is more stable than the MDF in all tests, but only in the 150 N axial test is the difference statistically significant

Only P values < 0.05 are displayed ('–' indicates no statistical significance)

Table 4 Axial and torsional failure test results

	Axial stiffnes					Torsional stiffness				
	N	Mean	SD ±	Min	Max	N	Mean	SD ±	Min	Max
Osteotomy type										
ABPobl	3	8,170	2,682	6,021	11,176	3	31.7	4.5	26.9	35.9
MDF	3	5,723	990	4,618	6,528	3	28.4	3.2	26.0	32.1
ASP	3	1,601	220	1,350	1,758	3	21.8	16.9	4*	37.3
LDF	3	3,197	895	2,227	3,989	3	23.9	18.3	3.2*	37.8
ABPperp	3	6,464	1,521	4,875	7,906	3	22.6	4.2	17.9	26.2

Results for the axial and torsional failure tests are shown; the number of femurs (N), mean stiffness and minimum and maximum are detailed. Axial stiffness is in N/mm and torsional stiffness in Nm/°

found highest in the ABPobl configuration (Table 4 and Fig. 4).

Torsional loading

No visible damage to bone, bone–implant construct or implant was found during the torsion tests. The lateral open SCO techniques (ASP and LDF) showed more motion compared with ABPobl and MDF (Table 2 and Fig. 5). Maximum motion was measured in all tests in ABPpp; it allowed statistically significantly more motion than the ABPobl and MDF in all tests (Table 3).

Torsional failure tests

In all medial closing-wedge SCO techniques, the opposing lateral cortex bone-bridge fractured first. Thereafter, in the ABPobl configuration, a subsequent spiral fracture occurred just proximal from the plate, whereas in ABPperp no fracture occurred, the proximal femur end kept turning clockwise, with bending of the screws at the screw–bone interface clearly visible (Fig. 6). In the MDF configuration, a fracture occurred at the screw–bone interface in all femurs (Fig. 6). In both ASP and LDF configurations, the opposite medial cortex fractured almost immediately after the start of the test in one femur (* in Table 4). Thereafter, in ASP, the proximal femur end kept turning inward as the plates themselves bend (Fig. 6). In LDF, subsequently, there was a spiral fracture just proximal of the plate in one femur, a spiral fracture that extended to the bone–screw interface in the second, and there was failure in the third because the screws were pulled out of the bone. Calculated stiffness was greatest in the ABPobl configuration (Table 4 and Fig. 7).

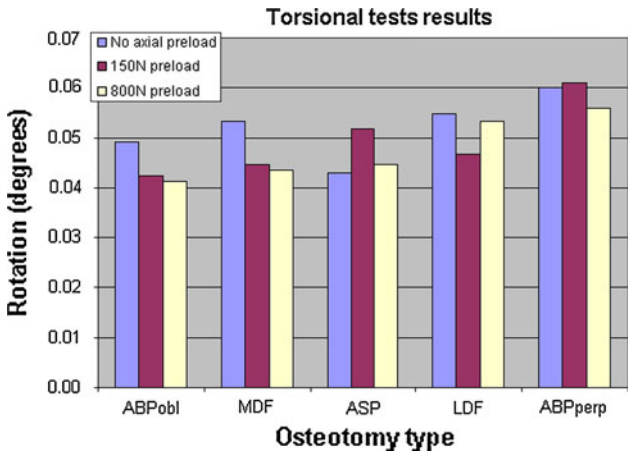

Fig. 4 Graphic view of the axial failure test results. Results for the axial failure tests; stiffness is displayed in Nm per millimetre displacement on the *Z*-axis

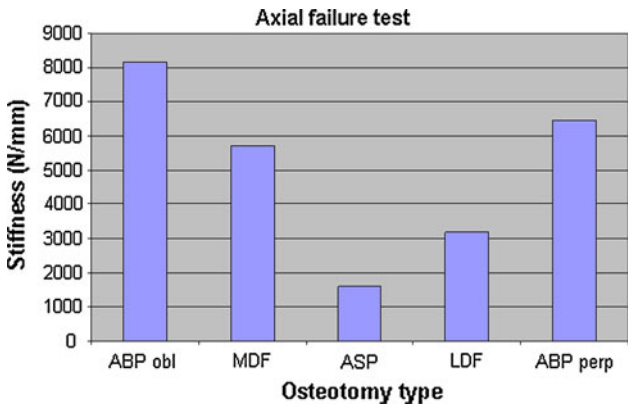

Fig. 5 Graphic view of the torsional test results. Results for the torsional test runs; results for each test are displayed for each modality; rotation is displayed in degrees rotation

Discussion

In this comparative biomechanical study, the oblique closing-wedge osteotomy with conventional angled blade plate and rigid compression was found to be the most stable configuration.

In the current study, an attempt was made to simulate physiological loading, unlike the non-physiological uniaxial stress and fatigue testing often done by the plate manufacturer. A physiological mechanical loading axis of 2° varus of the femur was used, the entire femur was loaded, loading was applied through the centre of the femoral head and loads simulating partial and full weight bearing were used in the axial loading tests. Furthermore, an attempt was made to simulate the natural torque moment that occurs during flexion–extension of the femur, during walking with partial and full weight bearing. It is the authors' opinion that the data provided in this study can therefore be used for decision-making in clinical practice regarding functional rehabilitation.

The superior stability and stiffness of the angled blade plate (ABPobl) when compared with the LCP (MDF) configuration is not unexpected. LCP plates in general act as an internal fixator, whereas the angled blade plate is compressed rigidly against the cortex allowing for less motion at the fracture site, or in the case of a SCO, the osteotomy. Subsequently, bone healing in LCP fixation is fundamentally different from bone healing with rigid fixation: secondary versus primary bone healing. The various biological advantages of LCP fixation versus rigid compression apply to LCP fixation in osteotomies [23]. The clinical use of angle-stable implants (LCP) in tibia osteotomies has been reported, and their biomechanical properties have been documented [1, 7, 19–21, 23]. The biomechanical properties of LCP used in SCO have, on the other hand, not been documented previously. Furthermore, exact comparison of bone-healing rates between LCP fixation and rigid fixation in SCO is not available. In this study, only the primary fixation strength in a composite femur model was tested. It is therefore unknown how the results in this study translate to actual bone-healing rates, loss of correction and clinical outcome in patients treated using LCP fixation in SCO.

The two opening-wedge plate and osteotomy configurations tested performed less well than the closing-wedge configurations. This may be due either to the biomechanical properties of the implant and the bone–implant construct or to the open wedge technique itself, with the lack of bone compression at the osteotomy site and a difference in load-bearing capacity of the bone bridge of the opposite cortex in open wedge when compared with closing-wedge SCO. The observed poor stiffness in the torsional failure tests in the two open-wedge techniques, with observed immediate fracture of the opposite cortex in both axial and torsional failure tests, suggests that the strength of the intact cortex plays a significant role in the stability of implants used in these plate and osteotomy configurations. In this study, the defect created by the open wedge osteotomy was not filled with a graft, which might influence the initial stability. This may lead to load sharing in axial and rotational testing of which the effects are unknown. In clinical use, grafts are primarily inserted to promote bone healing, and the contribution to initial stability of a graft is questionable. Until now, its use has only been recommended in larger defects. Franco et al. [6] using the spacer plate tested in this study recommended filling of the gap only if the defect was larger than 7.5 mm. In proximal open wedge tibia osteotomies, clinical results show that when an LCP is used for fixation, filling of the gap is not necessary to retain the achieved correction [2].

Fig. 6 Detailed view of the failure patterns in the torsional failure tests. Fracture of the femur at the screw–bone interface in the MDF in the torsional failure tests (*left*).The screws have clearly been bent at the screw–bone interface in the ABPperp in the torsional failure test (*middle*).The ASP itself has been bent in the torsional failure test (*right*)

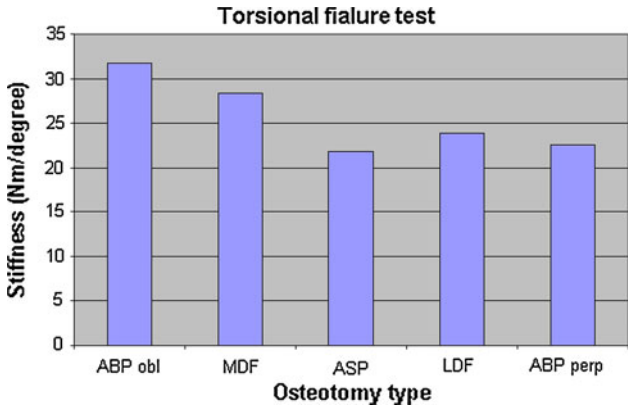

Fig. 7 Graphic view of the torsional failure test results. Results for the torsional failure tests; stiffness is displayed in Nm/degree rotation around the *Z*-axis

In this study, it was found that an oblique osteotomy is more stable than a perpendicular osteotomy. This is in accordance with the observation of Stahelin who suggested that a larger cortical contact area after closing of the wedge enhances stability [17]. The difference between perpendicular and oblique saw cuts became apparent in the torsional tests, the configuration with the perpendicular saw cut clearly showing less stability (Table 3).

In patients who undergo SCO, postoperative functional rehabilitation is paramount to regain knee function. Furthermore, maintaining the angle of correction is essential in obtaining good long-term clinical results. A bone–implant construct that has optimal biomechanical and biological fixation characteristics and allows for functional rehabilitation and partial to full weight bearing will improve clinical outcome in patients who undergo SCO. On the basis of the stability and stiffness found in this study, no clear recommendation for the use of LCP (MDF) over the rigid compression technique (ABPobl) can be made. From a surgical standpoint, as well as from the aforementioned biological standpoint, MDF has several advantages over the angled blade plate. Medial closing-wedge SCO with angled blade plate is a demanding surgical technique; it has been associated with complications including plate and screw failure, non-union, and loss of correction during bone healing [11, 13–17].

Fixation using MDF is a less demanding surgical procedure with better control of the amount of deformity correction and less complications [8]. Opening-wedge SCO techniques are technically even less demanding than the closing-wedge techniques and allow for precise deformity correction. However, in the present study, stability of fixation of the open-wedge techniques is significantly lower than the closing-wedge techniques. Additional stability can be provided by hinged orthoses, or a cast during functional rehabilitation that in the current authors' opinion should be performed at a slower rate than in closing-wedge techniques.

Future clinical studies will, however, have to prove all these supposed advantages, because to date no information on the long-term clinical results and the complications of the use of LCP in SCO is available. Important limitations of this study are the limited amount of femurs available for the failure tests; standard deviations are fairly large in these tests. There might not be enough data to draw definitive conclusions on the behaviour of the constructs in the failure tests. Test runs had to be limited to 100 cycles for practical reasons; data storage requirements would otherwise be too high. Furthermore, in an experimental setup like the one used, the effect of the soft tissues on stability and stiffness of course cannot be taken into account.

Conclusion

This experimental study presents baseline data on the differences in the primary stability of bone–implant constructs

used in SCO. The data in this study can be used as reference for future testing of SCO techniques. Furthermore, it is recommended that based on the differences found, the early postoperative rehabilitation protocol is tailored to the stability and stiffness of the fixation method used.

Acknowledgments The respective manufacturers provided all plates and screws; they had no influence on the study itself in any way, shape or form, however. No additional funding was received for this study.

References

1. Agneskirchner JD, Freiling D, Hurschler C, Lobenhoffer P (2006) Primary stability of four different implants for opening wedge high tibial osteotomy. Knee Surg Sports Traumatol Arthrosc 14:291–300
2. Brinkman JM, Lobenhoffer P, Agneskirchner JD, Staubli AE, Wymenga AB, van Heerwaarden RJ (2008) Osteotomies around the knee: patient selection, stability of fixation and bone healing in high tibial osteotomies. J Bone Joint Surg Br 90:1548–1557
3. Cusick RP, Lucas GL, McQueen DA, Graber CD (2000) Construct stiffness of different fixation methods for supracondylar femoral fractures above total knee prostheses. Am J Orthop 29:695–699
4. Dvir Z, Prushansky T (2000) Reproducibility and instrument validity of a new ultrasonography-based system for measuring cervical spine kinematics. Clin Biomech 15:658–664
5. Firoozbakhsh K, Behzadi K, DeCoster TA, Moneim MS, Naraghi FF (1995) Mechanics of retrograde nail versus plate fixation for supracondylar femur fractures. J Orthop Trauma 9:152–157
6. Franco V, Cipolla M, Gerullo G, Gianni E, Puddu G (2004) Open wedge osteotomy of the distal femur in the valgus knee. Orthopade 33:185–192
7. Frigg R (2003) Development of the locking compression plate. Injury 34(Supplement 2):6–10
8. van Heerwaarden RJ, Wymenga AB, Freiling D, Lobenhoffer P (2007) Distal medial closed wedge varus femur osteotomy stabilized with Tomofix plate fixator. Op Tech Orthopaedics 17:12–21
9. Heiner AD, Brown TD (2001) Structural properties of a new design of composite replicate femurs and tibias. J Biomech 34:773–781
10. Hsu RW, Himeno S, Coventry MB, Chao EY (1990) Normal axial alignment of the lower extremity and load-bearing distribution at the knee. Clin Orthop 90:215–227
11. Learmonth ID (1990) A simple technique for varus supracondylar osteotomy in genu valgum. J Bone Joint Surg Br 72:235–237
12. Luo CF (2004) Reference axes for reconstruction of the knee. Knee 11:251–257
13. Marti RK, Schröder J, Witteveen A (2000) The closed wedge varus supracondylar osteotomy. Oper Tech Sports Med 8:48–55
14. McDermott AG, Finklestein JA, Farine I, Boynton EL, MacIntosh DL, Gross A (1988) Distal femoral varus osteotomy for valgus deformity of the knee. J Bone Joint Surg Am 70:110–116
15. Miniaci A, Grossmann SP, Jakob RP (1990) Supracondylar femoral varus osteotomy in the treatment of valgus knee deformity. Am J Knee Surg 3:65–73
16. Miniaci A, Watson LW (2002) Distal femoral osteotomy. In: Fu FF (ed) Knee surgery, 1994. Williams & Wilkins, New York, pp 1173–1180
17. Stahelin T, Hardegger F, Ward JC (2000) Supracondylar osteotomy of the femur with use of compression Osteosynthesis with a malleable implant. J Bone Joint Surg Am 82:712–722
18. Stahelin T, Hardegger F (2004) Incomplete, supracondylar femur osteotomy. A minimally invasive compression osteosynthesis with soft implant. Orthopade 33:178–184
19. Staubli AE, De Simoni C, Babst R, Lobenhoffer P (2003) TomoFix: a new LCP-concept for open wedge osteotomy of the medial proximal tibia—early results in 92 cases. Injury 34(Suppl 2): 55–62
20. Stoffel K, Dieter U, Stachowiak G, Gachter A, Kuster MS (2003) Biomechanical testing of the LCP—how can stability in locked internal fixators be controlled? Injury 34(Suppl 2):11–19
21. Stoffel K, Stachowiak G, Kuster M (2004) Open wedge high tibial osteotomy: biomechanical investigation of the modified Arthrex Osteotomy Plate (Puddu Plate) and the TomoFix Plate. Clin Biomech 19:944–950
22. Szivek JA, Weng M, Karpman R (1990) Variability in the torsional and bending reponse of a commercially available composite "femur". J Appl Biomater 1:183–186
23. Wagner M (2003) General principles for the clinical use of the LCP. Injury 34(Suppl 2):31–42
24. Walsh JC, Quinlan JF, Stapleton R, FitzPatrick DP, McCormack D (2007) Three-dimensional motion analysis of the lumbar spine during "free squat" weight lift training. Am J Sports Med 35:927–932
25. Zlowodzki M, Williamson S, Cole PA, Zardiackas LD, Kregor PJ (2004) Biomechanical evaluation of the less invasive stabilization system, angled blade plate, and retrograde intramedullary nail for the internal fixation of distal femur fractures. J Orthop Trauma 8:494–502